

Diffusion of hydrogen in Ti–Zr–Ni quasicrystals

This article has been downloaded from IOPscience. Please scroll down to see the full text article.

2003 J. Phys.: Condens. Matter 15 5001

(<http://iopscience.iop.org/0953-8984/15/29/311>)

View [the table of contents for this issue](#), or go to the [journal homepage](#) for more

Download details:

IP Address: 171.66.16.121

The article was downloaded on 19/05/2010 at 14:19

Please note that [terms and conditions apply](#).

Diffusion of hydrogen in Ti–Zr–Ni quasicrystals

V Azhazha¹, A Grib^{2,4}, G Khadzhay², S Malikhin³, B Merisov² and A Pugachov³

¹ National Science Centre, Kharkov Institute of Physics and Technology, Akademicheskaya street 1, 61108 Kharkov, Ukraine

² Physics Department, Kharkov National University, Svobody sq. 4, 61077 Kharkov, Ukraine

³ National Technical University, Kharkov Polytechnical Institute, Frunze street 21, 61002 Kharkov, Ukraine

E-mail: Alexander.N.Grib@univer.kharkov.ua

Received 31 October 2002, in final form 12 May 2003

Published 11 July 2003

Online at stacks.iop.org/JPhysCM/15/5001

Abstract

We report the first straightforward measurements of the diffusion coefficient of hydrogen migrating in icosahedral (i-) quasicrystal ribbons of $\text{Ti}_{45}\text{Zr}_{38}\text{Ni}_{17}$ and in two-phase bulk samples containing both the i-phase and the Laves phase. It is found that at 273–353 K diffusion obeys Arrhenius's law with activation energy 0.24 eV and that the ratio of the volumes of the phases changes at hydrogenization.

1. Introduction

Hydrogen, because of its dimensions and mass, is the smallest dopant that can be used with metals. High values of the diffusion coefficient and the low activation energy of diffusion in crystalline metals can be caused by the quantum character of the motion of hydrogen in the lattice. An investigation of the process of hydrogen diffusion in quasiperiodical crystals (QC) could resolve the question of how the absence of translation invariance in their structure influences the characteristics of the diffusion of hydrogen.

Alloys of the system Ti–Zr–Ni containing the QC-phase have unique properties of the accumulation and desorption of hydrogen. In particular, the quasicrystal phase of $\text{Ti}_{45}\text{Zr}_{38}\text{Ni}_{17}$ has a ratio of the quantity of hydrogen atoms to atoms of the metal of $H/M = 1.7$ which is larger than that for LaNi_5 ($H/M = 1.1$) [1–5]. Data about the diffusion of hydrogen in Ti–Zr–Ni quasicrystals in the interval of the exploitation temperatures are necessary for the calculation of characteristic times of homogenization of the concentration of hydrogen along the volume, its sorption and desorption.

⁴ Author to whom any correspondence should be addressed.

2. Experiment

2.1. The samples

For obtaining ingots of nominal composition $\text{Ti}_{45}\text{Zr}_{38}\text{Ni}_{17}$, alloy ingots of the desired composition were first produced by arc melting mixtures of the pure elements in an argon atmosphere at a pressure of 10^5 Pa. The initial elements have been taken as follows: Ti (99.9% purity), Zr (99.9% purity), Ni (99.9% purity). The smelt and the frequent turning over of ingots provide homogenization of the composition and structure throughout their volume. Samples of two types were made from ingots. Ribbon samples with dimensions $2 \text{ cm} \times 1 \text{ mm}$ and thickness of about $40 \mu\text{m}$ were obtained by rapid quenching of the melt on a rolling copper disc. The linear velocity of the rolling disc was 20 m s^{-1} . Bulk ingots were cut from the analogous ingot in the form of bars with rectangular section $1 \times 1 \text{ mm}^2$ and with lengths of about 15 mm.

2.2. Analysis of the composition and the structure

The analysis of the chemical composition was carried out using x-ray fluorescence which showed that mean variations of the chemical composition of the samples were about 0.5%. The analysis of crystalline phases was carried out by a comparison of experimental data in the location of the diffraction peaks, 2θ and their intensity was compared with Powder Diffraction File [6] and also with [7, 8]. The identification of the quasicrystalline phase was performed as in [9–12], and indexes (N, M) were assigned according to the scheme given in [13]. As the parameters describing the quasicrystal structure, we used a lattice parameter in six-dimensional hypercubic reciprocal space, a_{6D} , related to the diffraction vector module Q by the following expression:

$$Q = \frac{2\pi \sin \theta}{\lambda} = \frac{2\pi}{a_{6D}} \sqrt{\frac{N + M\tau}{2(2 + \tau)}}, \quad (1)$$

as well as a parameter of quasicrystallinity in three-dimensional space related to a_{6D} by the expression

$$a_q = \frac{a_{6D}}{\sqrt{2}}, \quad (2)$$

where $\tau = 1.618 \dots$ is the irrational ‘gold number’. To describe the perfection of the structure of the quasicrystal phase, we used the coherence length, which was determined from the width of the diffraction peaks.

2.3. The investigation of diffusion

For measurements of diffusion of hydrogen we choose the experimental method based on the reproduction of boundary and initial conditions of the quasi-one-dimensional diffusion from one limit-sized bar into another:

$$\left. \frac{\partial C}{\partial x} \right|_{x=0,l} = 0, \quad C(x, 0) = \begin{cases} C_0, & 0 < x < h < l \\ 0, & h < x < l, \end{cases} \quad (3)$$

where C is the concentration of hydrogen, x is the coordinate along which the diffusion propagates, t is time, D is the diffusion coefficient, h is the coordinate of the boundary of the saturated part of the sample, l is the total length of the sample. These boundary conditions mean that there is no flux of hydrogen at the ends of the sample. The plot of the supposed initial distribution of hydrogen is shown in figure 1(a).

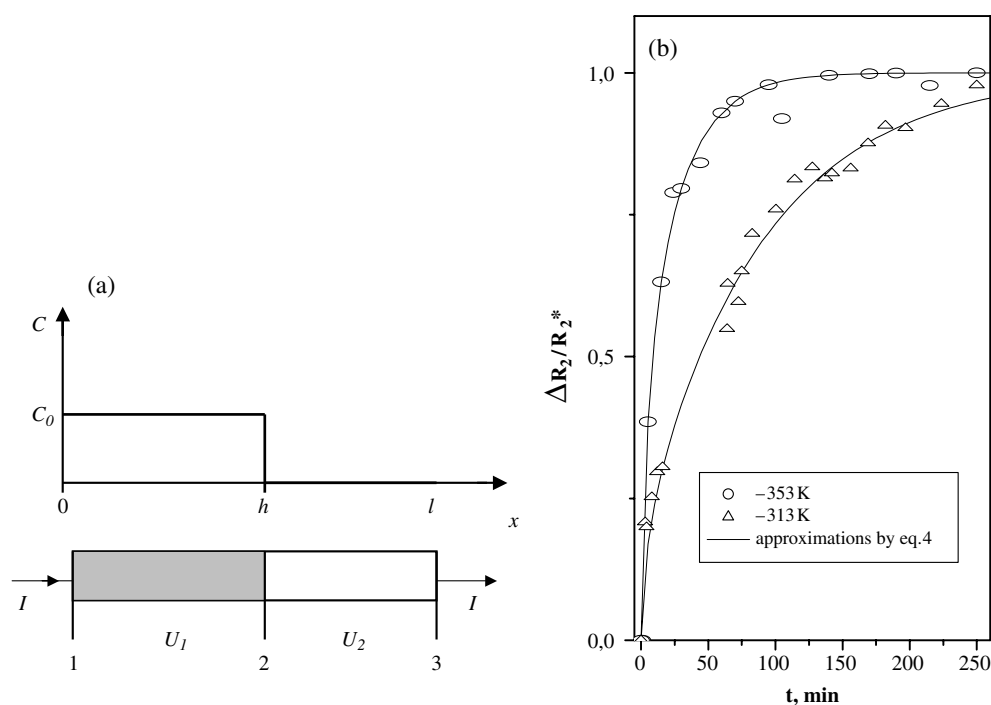


Figure 1. (a) Above: the scheme of the initial concentration profile $C(x)$ along the sample after saturation by hydrogen. Below: the scheme of the sample with electrical contacts where I is the current, U_1 and U_2 are voltage differences, 1, 2, 3 are potential contacts; the saturated part of the sample is shaded. (b) Time dependences of the normalized excess resistivity $\frac{\Delta R_2}{R_2^*}$, where $R_2^* = R_2(t = \infty)$ measured for temperatures 353 K (circles) and 313 K (triangles), lines are approximations by equation (4).

In the experiment, these initial conditions were created in the following way. Part of the sample was saturated electrolytically by hydrogen, i.e. approximately half of the length of the ribbon between potential contacts 1 and 2, excluding contact 2 itself (figure 1(a)), was plunged into the electrolyte and the saturation of this part occurred through surfaces of the sample over several minutes. The saturated part of the ribbon sample between the potential contacts 1 and 2 is shaded in this scheme. In the experiment, both current and potential contacts were glued to samples by the electrically conductive epoxy EPO-TEK H20E. In the process of gluing the contacts, samples were annealed at 373 K for 120 min. Measurements were made in the range 273–353 K.

We assume that hydrogen is distributed homogeneously along the volume of the plunged part of the sample and that the edge of the initial concentration profile of hydrogen is rectangular, though both of these conditions are slightly violated in the experiment. However, the role of these deviations is small because the hydrogen saturation time is much smaller than the time for the diffusion process.

The additional scattering of electrons on protons causes an increase of the electrical resistance of the saturated part of the sample. Thus, the electrical resistance of the measured part of the sample is proportional to the total mass of hydrogen in this part. Due to the migration of protons along the sample from the saturated part to the non-saturated part, the electrical resistance of the saturated part decreases whereas the electrical resistance of the non-saturated

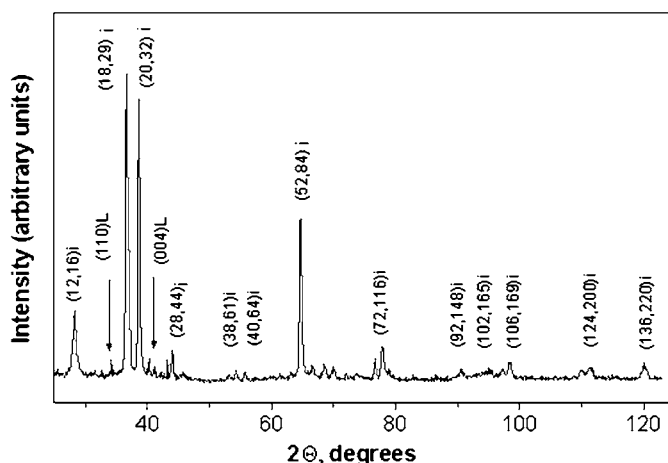


Figure 2. Diffraction pattern of speed-quenched ribbon $\text{Ti}_{45}\text{Zr}_{38}\text{Ni}_{17}$ with Cu $K\alpha$ radiation. L—the Laves phase (C14); i—the quasicrystalline icosahedral phase.

part increases. The time dependence of the quantity of hydrogen, $M(t)$, in the non-saturated part of the sample obtained from the solution of the diffusion equation with boundary and initial conditions (3) is as follows [14]:

$$M(t) = -D \int_0^l \left. \frac{\partial C(x,t)}{\partial x} \right|_{x=h} dx = A \sum_{n=1}^{\infty} \frac{1}{n^2} \sin^2 \frac{\pi n h}{l} \left[1 - \exp\left(-\frac{\pi^2 n^2 D t}{l^2}\right) \right], \quad (4)$$

where $A \approx \frac{2C_0 l}{\pi^2}$. It is supposed that the change of the resistance of the non-saturated part of the sample is proportional to the quantity of migrating hydrogen $R_2 \sim M(t)$ (see figures 1). Fitting equation (4) to the experimental data, one obtains the diffusion coefficient of hydrogen in the sample.

3. Results and discussion

3.1. The structure and phase composition of samples

The typical diffraction pattern of a ribbon sample is shown in figure 2. There is no amorphous phase in the samples. The main phase is a quasicrystalline icosahedral phase (i-phase) with quasilattice constant $a_q = 0.5188$ nm and the coherence length is 35–40 nm. The parameter a_q was calculated using positions of lines at high angles $2\theta = 110^\circ$ – 130° . The obtained values of a_q are in accordance with the results [2, 3, 15, 16]. Several lines of low intensity corresponding to Laves phase (L) TiZrNi (MgZn_2 structural type) were revealed as well [7–10, 15, 16]. The observed phase composition is in accordance with the equilibrium phase diagram for a Ti–Zr–Ni system [17, 18].

The estimation of phase volume parts in the composition can be carried out using the following considerations. The Laves phases, the approximant phases and the i-phase are related by the composition as well as by the structure [2, 3, 9–11, 15–21]. Transitions between these phases are possible as a result of rather small coordinated shifts of atoms [19, 22]. Therefore it can be supposed that in the first approximation the structure factor is the same for all mentioned phases. As simulations showed [19], changes of the integral intensity of diffraction lines are small if atomic shifts are small in comparison with the lattice parameter of the crystal (or with the parameter of quasicrystallinity). In this case the volume parts of phases

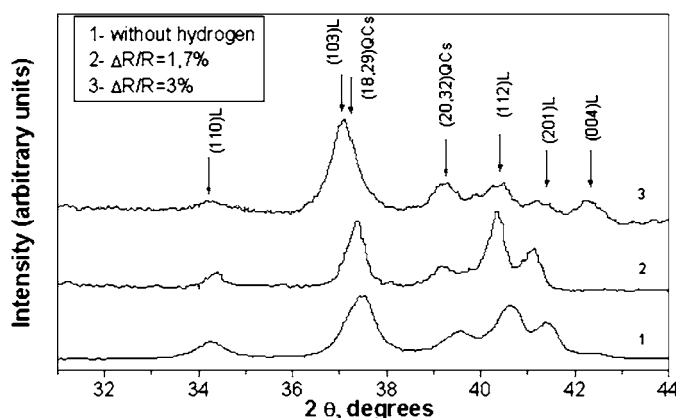


Figure 3. Diffraction pattern of a bulk sample with different extent of hydrogen saturation. (1) initial state; (2) $H/M \approx 0.06$, $\Delta R/R \approx 1, 7\%$; (3) $H/M \approx 0.08$, $\Delta R/R \approx 3\%$.

can be estimated using the ratio of integral intensities of closely disposed lines of different phases.

Using the ratio of integral intensities of the *i*-phase (20, 32) line and the line (112) of the *L*-phase in ribbons, we estimated that the averaged ratio between volume parts of the quasicrystalline *i*-phase and the Laves phase is 30:1.

The saturation of samples by hydrogen caused the shift of quasicrystal lines to lower angles and the decrease of intensities of lines. The concentration of hydrogen in ribbons estimated accordingly to the data [2, 3], reached $H/M \approx 0.26$. In some cases splitting of lines was observed in samples with higher content of Laves phase. This splitting can indicate the non-uniform hydrogen distribution in samples.

A typical diffraction pattern from a bulk sample is shown in figure 3. It is seen that the main phases are the Laves phase and the *i*-phase. The diffraction pattern is characterized by the overlap of the line (103) of the *L*-phase and the line (18, 29) of the *i*-phase. The quasilattice constant a_q in the initial (i.e. before hydrogenization) state was approximately 0.5114 nm; the coherence length was 8–10 nm, which is essentially smaller than that in ribbons. This indicates the more perfect structure of the quasicrystal phase in ribbons obtained by speed quenching. The ratio of volume parts of the *i*-phase and the Laves phase in bulk samples is 1:2.

As seen from figure 3, the saturation by hydrogen leads to the shift of all diffraction lines to smaller angles, which agrees with the observed data [1, 4, 15]. The quasilattice constant a_q increases by about 0.002 nm, which, according to the data [2, 3], corresponds to a concentration of hydrogen $H/M \approx 0.08$. The lattice parameters of the Laves phase vary in the following way: from 5.223 up to 5.246 Å, and *c* from 8.537 up to 8.580 Å. This corresponds to a linear increase of the volume of the Laves unit cell from 0.2018 to 0.2040 nm³ in this range of hydrogen concentrations. The ratio $c/a = 1.635$ remains constant, which indicates an isotropic expansion of the TiZrNi lattice under hydrogen saturation. Concentrations of hydrogen in the phases are comparable with each other.

It is necessary to note that the saturation by hydrogen causes an increase of the integral intensity of diffraction lines of the *i*-phase, for example (20, 32), relative to the intensity of the line (112) of the Laves phase. The analogous effect was observed in the saturation of powders [3] and rapidly quenched ribbons [15] of Ti–Zr–Ni alloys, however, this effect is not always unambiguous and monotone.

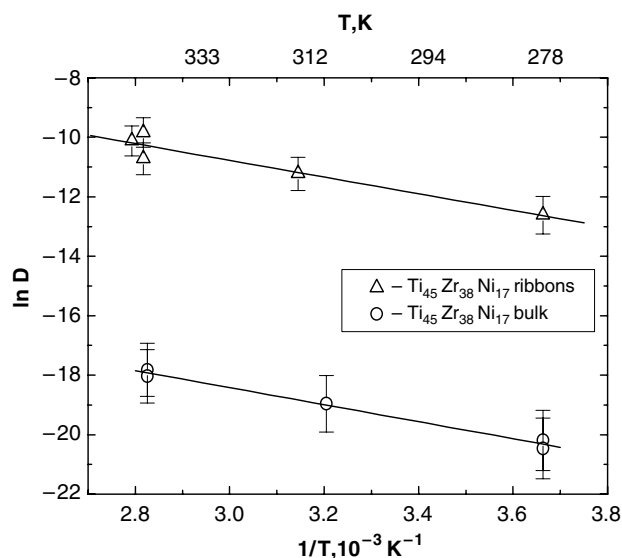


Figure 4. The dependence $\ln(D) = f(1/T)$ for $\text{Ti}_{45}\text{Zr}_{38}\text{Ni}_{17}$ ribbons (triangles) and bulk ingots (circles).

3.2. Diffusion of hydrogen

Changes of electrical resistivities $\Delta R_2 = R_2(t) - R_2(t = 0)$ (here $R_2(t = 0)$ are resistances of parts of the sample immediately after the saturation) of ribbons due to migrating hydrogen are plotted in figure 1(b) in normalized units together with approximations using equation (4). It is seen that the approximation from equation (4) is valid for our data.

Dependences of $\ln D$ on the reciprocal temperature $1/T$ for both ribbon and bulk samples are shown in figure 4. These dependences obey the Arrhenius law $D = D_0 \exp(-\frac{U}{k_B T})$, where k_B is the Boltzmann constant. For ribbons $D_0 = (1 \pm 0.4) \times 10^{-1} \text{ cm}^2 \text{ s}^{-1}$, $U = 0.24 \pm 0.04 \text{ eV}$; for bulk samples $D_0 = (5 \pm 0.2) \times 10^{-5} \text{ cm}^2 \text{ s}^{-1}$, $U = 0.25 \pm 0.02 \text{ eV}$.

The activation energies of diffusion $U = 0.24\text{--}0.25 \text{ eV}$ are almost the same for ribbons and bulk samples. The obtained values of U are lower than those calculated in [23–25] from data of nuclear spin–lattice relaxation rates and ultrasonic experiments on ribbons of Ti–Zr–Ni quasicrystals ($U = 0.35\text{--}0.41 \text{ eV}$). At the same time our data coincide with values of the activation energy of hydrogen obtained in diffusion experiments for Ti-based alloys [26, 27].

The value of the diffusion coefficient for bulk samples is comparable with that for amorphous metals ($\sim 10^{-8} \text{ cm}^2 \text{ s}^{-1}$ [28]). This is stipulated by the multiphase structure and the low quality of phases in these samples (see section 3.1 of this paper).

The large value of the coefficient D_0 in ribbons is non-trivial because the mean length of the jump b in ribbons calculated from the expression $D_0 \approx b^2 \nu$ (here $\nu = 5.8 \times 10^{12} \text{ s}^{-1}$ [24] is the phonon driven attempt frequency of the proton in the direction of the jump in Ti–Zr–Ni quasicrystals) is about 10 \AA . This value is equal to several mean distances between available proton sites in Ti–Zr–Ni quasicrystals [24]. Such a value of b could be explained in terms of the conception of delocalized states of the proton in the lattice [29, 30]. It was shown [29] that there is a fraction of delocalized protons in the lattice at room temperature. According to the quantum model [30], the proton is considered to be a wavepacket that can propagate through several neighbour interstitial sites in perfect crystal lattices, i.e. the mean length of the diffusion jump is about three or four interstitial sites. The quantum character of hydrogen

motion was assumed in Ti–Zr–Ni quasicrystals for the explanation of experimental data of nuclear spin–lattice relaxation rates [24]. According to our x-ray data, the icosahedric phase in ribbons is of high quality and therefore the existence of propagating wavepackets for the proton inside the Bergman cluster is a reasonable possibility.

4. Conclusions

We investigated the structure and the diffusion coefficient of hydrogen in both quasicrystal ribbons and bulk samples of $\text{Ti}_{45}\text{Zr}_{38}\text{Ni}_{17}$. X-ray analyses of samples showed that bulk samples have a two-phase composition: the icosahedral quasicrystal phase and the Laves phase. The ribbons consist of the icosahedral quasicrystal phase and insufficient traces of the Laves phase.

It was found that the saturation by hydrogen leads to an increase of the volume part of the quasicrystal phase at the expense of the Laves phase.

The diffusion coefficient was measured in the range 273–353 K. It was found that the temperature dependences of the diffusion coefficient obey the Arrhenius law. Values of the activation energy are very close to each other and equal 0.24 and 0.25 eV for the ribbons and bulk respectively. Values of pre-exponential factors are different and equal to $(1 \pm 0.4) \times 10^{-1} \text{ cm}^2 \text{ s}^{-1}$ for ribbons and $(5 \pm 0.2) \times 10^{-5} \text{ cm}^2 \text{ s}^{-1}$ for bulk samples.

Acknowledgment

This work was supported by Swiss National Science Foundation in ranges of Joint Research Project Nr 7UKPJ062171.

References

- [1] Kelton K F and Gibbons P C 1997 *MRS Bull.* **11** 69
- [2] Viano A M, Majzoub E H, Stroud R M, Kramer M J, Misture S T, Gibbons P C and Kelton K F 1998 *Phil. Mag. A* **78** 131
- [3] Nicula R, Jianu A, Biris A R, Lupu D, Manaila R, Devenui A, Kumpf C and Burkel E 1998 *Eur. Phys. J. B* **3** 1
- [4] Nicula R, Jianu A, Ponkratz U and Burkel E 2000 *Phys. Rev. B* **62** 8844
- [5] Gibbons P C and Kelton K F 1999 *Toward industrial applications Physical Properties of Quasicrystals* ed Z M Stadnik (Berlin: Springer)
- [6] *Powder Diffraction File. Inorganic Sets* 1988 (Swarthmore, PA: International Centre for Diffraction Data)
- [7] Teslyuk M Yu 1969 *Metal Combinations With Structure of Laves Phases* (Moscow: Nauka) (in Russian)
- [8] Pirson U 1977 *Crystal Chemistry, Physics of Metals and Alloys* (Moscow: Mir) (in Russian)
- [9] Kelton K F, Kim W J and Stroud R M 1997 *Appl. Phys. Lett.* **70** 3230
- [10] Yi S and Kim D H 2000 *J. Mater. Res.* **15** 892
- [11] Lu P J, Deffeyes K, Steinhardt P J and Nan Yao 2001 *Phys. Rev. Lett.* **87** 275507-1
- [12] Kim W J and Kelton K F 1996 *Phil. Mag. Lett.* **74** 439
- [13] Cahn J W, Shechtman D and Gratias D 1986 *J. Mater. Res.* **1** 13
- [14] Herzricken C D and Dekhtyar I Ya 1960 *Diffusion in Metals and Alloys in a Solid Phase* (Moscow: Physical and Mathematical Publishing House) (in Russian)
- [15] Stroud R M, Kelton K F and Misture S T 1997 *J. Mater. Res.* **12** 434
- [16] Kim W J, Gibbons P C, Kelton K F and Yelon W B 1998 *Phys. Rev. B* **58** 2578
- [17] Henning R G, Carlsson A E, Kelton K F and Henley C L 2002 *Preprint cond-mat/0205202*
- [18] Davis J P, Majzoub E H, Simmons J M and Kelton K F 2000 *Mater. Sci. Eng.* **294–296** 104
- [19] Henning R G, Kelton K F, Carlsson A E and Henley C L 2002 *Preprint cond-mat/0202517*
- [20] Stroud R M, Viano A M, Gibbons P C and Kelton K F 1996 *Appl. Phys. Lett.* **69** 2998
- [21] Kim W J, Gibbons P C and Kelton K F 1997 *Phil. Mag. Lett.* **76** 199
- [22] Roshal' S B 2001 *Phys. Tverd. Tela* **43** 1884 (in Russian)
- [23] Foster K, Leisure R G, Shaklee J B, Kim J Y and Kelton K F 2000 *Phys. Rev. B* **61** 241

-
- [24] Shastri A, Majzoub E H, Borsa F, Gibbons P C and Kelton K F 1998 *Phys. Rev. B* **57** 5148
 - [25] McDowell A F, Adolphi N L and Sholl C A 2001 *J. Phys.: Condens. Matter* **13** 9799
 - [26] Holman W R, Crawford R W and Parese F 1965 *Trans. Metall. Soc. AIME* **233** 1836
 - [27] Kolachev B A, Nazimov O P and Zhuravlev L N 1969 *Izv. Vyssh. Uchebn. Zaved., Tsvetn. Metall.* **4** 104
 - [28] Kirchheim R 1982 *Acta Metall.* **30** 1069
 - [29] Oates W A, Mainwood A and Stoneham A M 1978 *Phil. Mag.* **38** 607
 - [30] Sussmann J A and Weissman Y 1972 *Phys. Status Solidi b* **53** 419